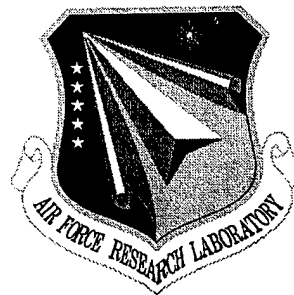


**AFRL-SN-RS-TR-2001-78**  
**Final Technical Report**  
**May 2001**



**NOVEL SPACE-TIME ADAPTIVE PROCESSING  
METHODS FOR GAUSSIAN AND NON-GAUSSIAN  
RADAR CLUTTER**

**ARCON Corporation**

**Muralidhar Rangaswamy**

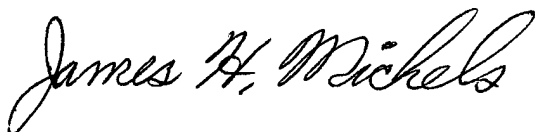
*APPROVED FOR PUBLIC RELEASE; DISTRIBUTION UNLIMITED.*

**20010607 021**

**AIR FORCE RESEARCH LABORATORY  
SENSORS DIRECTORATE  
ROME RESEARCH SITE  
ROME, NEW YORK**

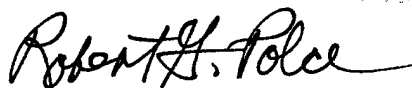
This report has been reviewed by the Air Force Research Laboratory, Information Directorate, Public Affairs Office (IFOIPA) and is releasable to the National Technical Information Service (NTIS). At NTIS it will be releasable to the general public, including foreign nations.

AFRL-SN-RS-TR-2001-78 has been reviewed and is approved for publication.



APPROVED: JAMES H. MICHELS  
Project Engineer

FOR THE DIRECTOR:



ROBERT G. POLCE  
Chief, Rome Operations Office  
Sensors Directorate

If your address has changed or if you wish to be removed from the Air Force Research Laboratory Rome Research Site mailing list, or if the addressee is no longer employed by your organization, please notify AFRL/SNRT, 26 Electronic Pky, Rome, NY 13441-4514. This will assist us in maintaining a current mailing list.

Do not return copies of this report unless contractual obligations or notices on a specific document require that it be returned.

**REPORT DOCUMENTATION PAGE**

Form Approved  
OMB No. 0704-0188

Public reporting burden for this collection of information is estimated to average 1 hour per response, including the time for reviewing instructions, searching existing data sources, gathering and maintaining the data needed, and completing and reviewing the collection of information. Send comments regarding this burden estimate or any other aspect of this collection of information, including suggestions for reducing this burden, to Washington Headquarters Services, Directorate for Information Operations and Reports, 1215 Jefferson Davis Highway, Suite 1204, Arlington, VA 22202-4302, and to the Office of Management and Budget, Paperwork Reduction Project (0704-0188), Washington, DC 20503.

1. AGENCY USE ONLY (Leave blank)	2. REPORT DATE MAY 2001	3. REPORT TYPE AND DATES COVERED Final Dec 98 - Oct 00
----------------------------------	----------------------------	---

4. TITLE AND SUBTITLE NOVEL SPACE-TIME ADAPTIVE PROCESSING METHODS FOR GAUSSIAN AND NON-GAUSSIAN RADAR CLUTTER	5. FUNDING NUMBERS C - F30602-98-C-0283 PE - 61102F PR - 2304 TA - E8 WU - PK
---	--

6. AUTHOR(S) Dr. Muralidhar Rangaswamy	
---	--

7. PERFORMING ORGANIZATION NAME(S) AND ADDRESS(ES) ARCON Corporation 260 Bear Hill Rd Waltham MA 02451-1080	8. PERFORMING ORGANIZATION REPORT NUMBER  N/A
--	---

9. SPONSORING/MONITORING AGENCY NAME(S) AND ADDRESS(ES) AFRL/SNRT 26 Electronic Pky Rome NY 13441-4514	10. SPONSORING/MONITORING AGENCY REPORT NUMBER  AFRL-SN-RS-TR-2001-78
---	---

11. SUPPLEMENTARY NOTES  Air Force Research Laboratory Project Engineer: Dr. James H. Michels, SNRT, 315-330-4432
---

12a. DISTRIBUTION AVAILABILITY STATEMENT Approved for public release: distribution unlimited.	12b. DISTRIBUTION CODE
--	------------------------

13. ABSTRACT (Maximum 200 words)

Our work on this contract has four main thrusts. We addressed (1) the problem of optimal target detection of a rank one signal in additive non-Gaussian clutter modeled as a spherically invariant random process. Performance analysis of the optimal signal processor was carried out. However, practical implementation of the optimal processor requires knowledge of the probability density function underlying the clutter, which is often unavailable. Hence, (2) we considered the performance of sub-optimum as well as ad-hoc approximations to the optimal processor. Next, (3) we concerned ourselves with the performance of parametric space-time adaptive processing methods in Gaussian interference and addressed issues of detection probability, constant false alarm rate and reduced training data support. Finally, (4) we provided a rigorous statistical analysis of the recently proposed non-homogeneity detector, which is useful for training data selection in STAP applications.

14. SUBJECT TERMS STAP, SIRV, K-distribution, CFAR, Probability of Detection, PAMF, NAMF, N-PAMF, Kelly GLRT, AMF, SINR, Multichannel AR, NHD, GIP, F-distribution, Beta distribution, Goodness-of-fit test	15. NUMBER OF PAGES 44
	16. PRICE CODE

17. SECURITY CLASSIFICATION OF REPORT UNCLASSIFIED	18. SECURITY CLASSIFICATION OF THIS PAGE UNCLASSIFIED	19. SECURITY CLASSIFICATION OF ABSTRACT UNCLASSIFIED	20. LIMITATION OF ABSTRACT UL
---	--	---	----------------------------------

# Contents

<b>1</b>	<b>Optimal Space-Time Adaptive Processing Method in Non-Gaussian Radar Clutter Backgrounds</b>	<b>1</b>
1.1	Motivation . . . . .	1
1.2	Problem Statement . . . . .	2
1.3	Performance Evaluation . . . . .	4
1.4	Conclusions . . . . .	6
<b>2</b>	<b>Analytical Expressions for the NMF and NAMF Tests</b>	<b>8</b>
2.1	Test Statistic Descriptions . . . . .	8
2.1.1	Non-Adaptive Test Statistics . . . . .	8
2.1.2	Adaptive Test Statistics . . . . .	9
2.2	Analytic Results . . . . .	9
2.3	Performance Results . . . . .	13
2.4	Summary . . . . .	15
<b>3</b>	<b>Statistical Analysis of the Nonhomogeneity Detector</b>	<b>17</b>
3.1	Introduction . . . . .	17
3.2	GIP Statistics: Known Covariance . . . . .	17
3.3	GIP Statistics: Unknown Covariance . . . . .	18
3.4	New Test for Nonhomogeneity . . . . .	20
3.5	Performance Analysis . . . . .	21
3.6	Conclusion . . . . .	21
	<b>Appendix A: Stochastic Representation for the Normalized GIP</b>	<b>29</b>

# List of Figures

1.1	Probability of detection vs Signal-to-noise-ratio $P_{fa} = 10^{-4}$ . . . . .	6
1.2	Probability of detection vs Signal-to-noise-ratio $P_{fa} = 10^{-4}$ . . . . .	7
2.1	NMF performance in K-distributed SIRP disturbance . . . . .	14
2.2	Threshold versus Shape Parameter . . . . .	14
2.3	NAMF Performance in Gaussian Clutter . . . . .	15
2.4	NAMF, Kelly GLRT, CFAR-AMF Performance in Gaussian Clutter . . . .	16
3.1	PDF of the normalized GIP . . . . .	22
3.2	Theoretical and empirical CDF of the normalized GIP . . . . .	22
3.3	Histogram of empirical data and theoretical PDF of the normalized GIP .	23
3.4	Type-I error versus threshold . . . . .	23
3.5	Normalized GIP vs Range . . . . .	24

# Acknowledgments

The author is thankful to Drs. J.H. Michels and B. Himed of the U.S. Air Force Research Laboratory, Dr. J.R. Roman of the Scientific Studies Corporation and Dr. K. Gerlach of the Naval Research Laboratory for their insightful comments and stimulating technical discussions. The author is especially grateful to Drs. B. Himed, J.H. Michels, and J.R. Roman for their collaborative efforts on several conference and journal publications.

# Executive Summary

This research effort represents our investigation on the following problems:

1. Optimal processor structure for detecting a rank one signal in additive non-Gaussian radar modeled by a spherically invariant random process (SIRP) and its performance analysis.
2. Analytical expressions for the detection and false alarm probability for two important detection tests.
3. Statistical analysis of the non-homogeneity detector for Gaussian interference scenarios.

Our work on item 1 presents integral expressions for detection and false alarm probabilities of the optimal processor for detecting a rank one signal in a background of non-Gaussian clutter which is modeled by a SIRP. It is well known that when operating in Gaussian clutter backgrounds, the best achievable performance is that of a matched filter (MF) or a normalized correlator. In this work we present the performance analysis of the corresponding optimal processor for SIRPs. Integral expressions for detection and false alarm probabilities are obtained [1].

In many instances, it is impossible to implement the optimal processor outlined in item 1. Consequently, we seek methods which circumvent the need to know the clutter probability density function (PDF). This aspect is addressed in item 2, where we present analytical results for the probability of detection and probability of false alarm for the normalized matched filter (NMF) and normalized adaptive matched filter (NAMF) tests. Performance is compared to the adaptive matched filter and the Kelly GLRT receiver. The analytic expressions derived in this work were reported in [2].

Finally, an important issue in STAP is that of homogeneity of training data. Non-homogeneity of the training data has a deleterious effect on STAP performance in that undernulled clutter significantly degrades detection and false alarm characteristics. Previous work in this area has proposed the use of a non-homogeneity detector (NHD) based on a generalized inner product (GIP). Our work on item 3 considers the statistical analysis of the NHD for Gaussian interference statistics. We show that a more stringent test can be constructed by accounting for the statistics of the (GIP) under the condition of finite training data support. In particular, exact theoretical expressions for the GIP PDF and GIP mean are derived. Additionally, we show that for Gaussian interference statistics,

the GIP admits a simple representation as the ratio of two statistically independent Chi-Square distributed random variables. Performance analysis of the more stringent GIP based test is presented. Results from this investigation were reported in [3].

# Chapter 1

## Optimal Space-Time Adaptive Processing Method in Non-Gaussian Radar Clutter Backgrounds

### 1.1 Motivation

This analysis is motivated by the problem of space-time adaptive (STAP) processing in non-Gaussian clutter backgrounds. The problem of adaptive target detection in Gaussian clutter has received considerable attention [4–8]. The corresponding problem for non-Gaussian clutter backgrounds has been the focus of recent work reported in [9–14]. The receiver developed in [7, 15] is an adaptive matched filter (AMF), whose performance asymptotically reaches that of the matched filter (MF) which is the optimal processor for Gaussian clutter statistics. Thus, the MF represents an upper bound on the performance of the AMF for Gaussian clutter statistics.

In [10, 11], we showed that the receiver for non-Gaussian SIRPs is equivalent to an adaptive matched filter compared to a data dependent threshold. The distribution of the test statistic was extremely difficult to derive in closed form. Consequently, performance analysis in [11] was carried out by Monte-Carlo simulation in the multichannel signal processing system developed at AFRL/SNRT. The goal of this effort is to obtain an upper bound on the performance of the adaptive processor provided by the optimal receiver for SIRPs. This enables the specification of meaningful adaptive performance metrics such as the sample support size needed to get to within 3dB of the optimal processor performance.

Accordingly, we briefly outline the derivation of the optimal processor for SIRPs and present relevant details of the performance evaluation. Integral expressions for the probability of detection and false alarm are derived. As a special case, these expressions reduce to the well known Gaussian MF results.

## 1.2 Problem Statement

We consider the following statistical hypothesis testing problem:

$$\begin{aligned} H_0 : \mathbf{x} &= \mathbf{y} \\ H_1 : \mathbf{x} &= a\mathbf{s} + \mathbf{y} \end{aligned} \quad (1.1)$$

where  $\mathbf{x} \equiv$  Received  $JN \times 1$  complex observation vector

$\mathbf{s} \equiv$  Known steering vector

$a \equiv$  Unknown complex signal amplitude

$\mathbf{y} \equiv$  Complex spherically invariant random vector (SIRV) with known Hermitian positive definite covariance matrix,  $\Sigma$  and known characteristic probability density function (PDF)  $f_V(v)$ . It is important to note that the optimal processor for SIRVs assumes knowledge of the covariance matrix and the characteristic PDF.

The maximum likelihood estimate of  $a$  is given by [11]

$$\hat{a} = \frac{\mathbf{s}^H \Sigma^{-1} \mathbf{x}}{\mathbf{s}^H \Sigma^{-1} \mathbf{s}} \quad (1.2)$$

This estimate is then used in a likelihood ratio test to discriminate between the two hypotheses. The likelihood ratio test for SIRPs takes on the form

$$\Lambda(\mathbf{x}) = \frac{h_{2JN}(q_1) \stackrel{H_1}{>}}{h_{2JN}(q_0) \stackrel{H_0}{<}} T \quad (1.3)$$

where  $q_0 = \mathbf{x}^H \Sigma^{-1} \mathbf{x}$ ,  $q_1 = \mathbf{x}^H \Sigma^{-1} \mathbf{x} - \frac{|\mathbf{s}^H \Sigma^{-1} \mathbf{x}|^2}{\mathbf{s}^H \Sigma^{-1} \mathbf{s}}$  and

$$h_{2JN}(q) = \int_0^\infty v^{-2JN} \exp(-\frac{q}{v^2}) f_V(v) dv. \quad (1.4)$$

Using  $\rho^2 = \frac{|\mathbf{s}^H \Sigma^{-1} \mathbf{x}|^2}{\mathbf{s}^H \Sigma^{-1} \mathbf{x} \mathbf{x}^H \Sigma^{-1} \mathbf{x}}$ , the magnitude squared coherence between  $\mathbf{s}$  and  $\mathbf{x}$ ,  $q_1$  is expressed as  $q_1 = q_0(1 - \rho^2)$ . Since SIRVs are closed under linear transformations, rotational and scaling operations on every SIRV result in another SIRV having the same characteristic PDF [16]. In all detection analyses involving colored noise spectra, there is no performance penalty for whitening the noise. Accordingly, we use an eigenvalue decomposition of the covariance matrix of the form  $\Sigma = \mathbf{E} \mathbf{D} \mathbf{E}^H$ , where  $\mathbf{E} \equiv$  Matrix whose columns are orthonormal eigenvectors of  $\Sigma$  and  $\mathbf{D}$  is the diagonal matrix of eigenvalues of  $\Sigma$ . Let  $\mathbf{D}^{-1/2} \mathbf{E}^H \mathbf{x} = \mathbf{x}'$  and  $\mathbf{D}^{-1/2} \mathbf{E}^H \mathbf{s} = \mathbf{s}'$ . From the closure property of SIRVs it follows that  $\mathbf{x}'$  is an SIRV with zero mean, identity ( $JN \times JN$ ) covariance matrix and characteristic PDF  $f_V(v)$ .

Consequently,

$$\begin{aligned} q_0 &= \|\mathbf{x}'\|^2 = \mathbf{x}^H \Sigma^{-1} \mathbf{x} \\ q_1 &= \|\mathbf{x}'\|^2 (1 - \rho^2) \\ \rho'^2 &= \frac{|\mathbf{s}'^H \mathbf{x}'|^2}{\mathbf{s}'^H \mathbf{s}' \mathbf{x}'^H \mathbf{x}'} \\ \|\mathbf{s}'\|^2 &= \mathbf{s}^H \Sigma^{-1} \mathbf{s} \end{aligned} \quad (1.5)$$

where  $\|\cdot\|^2$  denotes the squared norm.

We then define an additional transformation  $A$  which rotates  $\mathbf{s}'$  and places the signal energy into the first component of the rotated vector. More precisely let  $\mathbf{s}_0 = \mathbf{A}\mathbf{s}'$  where  $\mathbf{s}_0 = \|\mathbf{s}'\| [1, 0, \dots, 0]^T$ . The matrix  $\mathbf{A}$  is specified by the Householder transformation as  $\mathbf{A} = \mathbf{I} - 2 \frac{\mathbf{u}\mathbf{u}^H}{\|\mathbf{u}\|^2}$  where  $\mathbf{u} = (\mathbf{s}' - \mathbf{s}_0)$ . Let  $\mathbf{x}_0 = \mathbf{A}\mathbf{x}'$ . The following properties of  $\mathbf{A}$  can be readily established. For the sake of completeness, the proofs are provided here although they may be found elsewhere [17].

1.  $\mathbf{A}$  is a Hermitian symmetric matrix, i.e.,  $\mathbf{A} = \mathbf{A}^H$ .

Proof:

$$\mathbf{A}^H = [\mathbf{I} - 2 \frac{\mathbf{u}\mathbf{u}^H}{\|\mathbf{u}\|^2}]^H = \mathbf{I} - 2 \frac{\mathbf{u}\mathbf{u}^H}{\|\mathbf{u}\|^2} = \mathbf{A}$$

2.  $\mathbf{A}$  is a Unitary matrix. Thus,  $\mathbf{A}\mathbf{A}^H = \mathbf{A}^H\mathbf{A} = \mathbf{I}$ .

Proof:

From property 1, we have  $\mathbf{A} = \mathbf{A}^H$ . Hence,  $\mathbf{A}\mathbf{A}^H = \mathbf{A}^H\mathbf{A} = [\mathbf{I} - 2 \frac{\mathbf{u}\mathbf{u}^H}{\|\mathbf{u}\|^2}][\mathbf{I} - 2 \frac{\mathbf{u}\mathbf{u}^H}{\|\mathbf{u}\|^2}] = \mathbf{I} - 4 \frac{\mathbf{u}\mathbf{u}^H}{\|\mathbf{u}\|^2} + 4 \frac{\mathbf{u}\mathbf{u}^H}{\|\mathbf{u}\|^2} = \mathbf{I}$ .

3. The Householder transformation is norm preserving.

Proof:

We have  $\mathbf{s}_0 = \mathbf{A}\mathbf{s}'$ . Hence,  $\|\mathbf{s}_0\|^2 = \mathbf{s}'^H \mathbf{A}^H \mathbf{A} \mathbf{s}' = \|\mathbf{s}'\|^2$  (since  $\mathbf{A}^H \mathbf{A} = \mathbf{I}$  from property 2).

4. The inner product between two vectors undergoing the same Householder transformation remains unchanged.

Proof:

$$\mathbf{s}_0^H \mathbf{x}_0 = [\mathbf{A}\mathbf{s}']^H \mathbf{A}\mathbf{x}' = \mathbf{s}'^H \mathbf{A}^H \mathbf{A} \mathbf{x}' = \mathbf{s}'^H \mathbf{x}' \text{ (since } \mathbf{A}^H \mathbf{A} = \mathbf{I} \text{ from property 2).}$$

We use properties 3 and 4 of the Householder transformation to rewrite  $q_0$  and  $q_1$  as

$$\begin{aligned} q_0 &= \|\mathbf{x}'\|^2 = \|\mathbf{x}_0\|^2 = \sum_{i=1}^{JN} |X_{0i}|^2 \\ q_1 &= \|\mathbf{x}'\|^2 (1 - \rho'^2) = \|\mathbf{x}_0\|^2 (1 - \frac{|X_{01}|^2}{\|\mathbf{x}_0\|^2}) = \sum_{i=2}^{JN} |X_{0i}|^2. \end{aligned} \quad (1.6)$$

It is also worthwhile noting that  $\mathbf{x}_0$  is also an SIRV with zero mean, identity covariance matrix and characteristic PDF  $f_V(v)$ . Let  $W = |X_{01}|^2$  and  $\Delta = \sum_{i=2}^{JN} |X_{0i}|^2$ . As a result, the test of eq (1.3) reduces to

$$\Lambda(\mathbf{x}) = \frac{h_{2JN}(\Delta)}{h_{2JN}(W + \Delta)} \stackrel{H_1}{>} \underset{H_0}{<} T \quad (1.7)$$

which can equivalently be expressed as

$$W \stackrel{H_1}{>} \underset{H_0}{<} h_{2JN}^{-1}[\frac{1}{T} h_{2JN}(\Delta)] - \Delta \quad (1.8)$$

Let  $T^* = h_{2JN}^{-1}[\frac{1}{T} h_{2JN}(\Delta)] - \Delta$ . This reveals that the optimal strategy for detecting known signals (with unknown complex amplitude) in SIRPs (with known covariance matrix) is

equivalent to a matched filter compared to a data dependent threshold. The test of the form of eq (1.8) is convenient for carrying out performance analyses since it enables us to exploit the statistical independence between  $W$  and  $\Delta$  conditioned on  $V$ . This becomes clear in the next section.

The advantage of the Householder transformation is that it affords a dimensionality reduction by using a signal vector representation, in which all the signal energy is contained in the first component of the transformed signal vector. The remaining components of the transformed signal vector are zero. The Householder transformation also enables us to demonstrate the maximal invariance of the test statistic of eq (1.3) with respect to rotation and scaling transformations and hence, establish the constant false alarm rate (CFAR) feature of the test.

### 1.3 Performance Evaluation

In this section, we derive integral expressions for the probability of detection and false alarm for the test of eq (1.8). Since  $\mathbf{x}_0$  is an SIRV with zero mean and identity covariance matrix, it can be represented as the product of a complex-Gaussian random vector  $\mathbf{z}$  having zero mean and identity covariance matrix and a statistically independent nonnegative random variable  $V$  with PDF  $f_V(v)$  [18]. Thus,  $\mathbf{x}_0 = \mathbf{z}V$ . Consequently, under the  $H_0$  hypothesis, conditioned on  $V$ ,  $W$  and  $\Delta$  are statistically independent Chi-Squared distributed random variables with 1 and  $JN - 1$  complex degrees of freedom, respectively. Furthermore, the PDF of  $\Delta$  remains unchanged under the  $H_1$  hypothesis. Consequently,

$$f_{W|V}(w|v) = \frac{1}{v^2} \exp\left(-\frac{w}{v^2}\right) \quad w > 0 \quad (1.9)$$

$$f_{\Delta|V}(\Delta|v) = \frac{\Delta^{JN-2}}{\Gamma(JN-1)v^{2JN-2}} \exp\left(-\frac{\Delta}{v^2}\right) \quad \Delta > 0. \quad (1.10)$$

The false alarm probability,  $P_{fa}$ , of the test of eq (1.8) conditioned on  $\Delta$  and  $V$  is given by

$$P_{fa|\Delta,V} = \int_{T^*}^{\infty} \frac{1}{v^2} \exp\left(-\frac{w}{v^2}\right) dw = \exp\left(-\frac{T^*}{v^2}\right). \quad (1.11)$$

The unconditional false alarm probability is obtained as

$$P_{fa} = \int_0^{\infty} \int_0^{\infty} \exp\left(-\frac{T^*}{v^2}\right) f_{\Delta|V}(\Delta|v) f_V(v) d\Delta dv. \quad (1.12)$$

Under the  $H_1$  hypothesis, the PDF of  $\Delta$  conditioned on  $V$  remains unchanged. However, under  $H_1$ ,  $W$  is recognized to be the squared magnitude of a complex Gaussian random variable with mean  $\eta = |\hat{a}| \sqrt{\mathbf{s}^H \boldsymbol{\Sigma}^{-1} \mathbf{s}}$ . Hence,  $W$  conditioned on  $V$  is simply the square of a Rician distributed random variable  $R$ , whose PDF is given by

$$f_R(r) = \frac{2r}{v^2} \exp\left[-\frac{(r^2 + \eta^2)}{v^2}\right] I_0\left(\frac{2\eta r}{v^2}\right) \quad r > 0 \quad (1.13)$$

where  $I_0(\cdot)$  is the modified Bessel function of the first kind of order zero. Hence, the conditional probability of detection is given by

$$P_{D|\Delta,V} = \int_{\sqrt{T^*}}^{\infty} f_R(r) dr. \quad (1.14)$$

The unconditional probability of detection is obtained as

$$P_D = \int_0^{\infty} \int_0^{\infty} P_{D|\Delta,V} f_{\Delta|V}(\Delta|v) f_V(v) d\Delta dv. \quad (1.15)$$

Unfortunately, it is not possible to further simplify the integrals in eqs (1.12) and (1.15). Consequently, the integrals must be evaluated using numerical techniques. We consider the special case of Gaussian clutter. Then,  $h_{2JN}(q) = \exp(-q)$ , and  $f_V(v) = \delta(v - 1)$ . Consequently,  $T^* = h_{2JN}^{-1}[\frac{1}{T} h_{2JN}(\Delta)] - \Delta = \ln(T) = T_G$  (say). For this special case, the data dependence of  $T^*$  disappears. Using these observations in eq (1.12) and simplifying, it follows that  $P_{fa} = \exp(-T_G)$ . Using  $h_{2JN}(\cdot) = \exp(-\cdot)$ ,  $f_V(v) = \delta(v - 1)$  and  $T^* = T_G$  in eq (1.15), we see that the resulting probability of detection is given by

$$P_D = \int_{\sqrt{T^*}}^{\infty} 2r \exp[-(r^2 + \eta^2)] I_0(2\eta r) dr. \quad (1.16)$$

This is the well known expression for the matched filter detection probability.

We now generalize the analysis to allow for the complex signal amplitude to be a random variable. More precisely, we assume that  $a$  is a complex-Gaussian random variable with zero mean and variance  $\sigma^2$ . We then derive the performance of the test of eq (1.8) for this case.

Proceeding as before, it follows that the PDFs of  $W$  and  $\Delta$  under the  $H_0$  condition remain unchanged. Furthermore, the invariance of the PDF of  $\Delta$  under  $H_1$  is also preserved. It is worthwhile noting that the complex Gaussian distribution on the signal amplitude is also preserved after the Householder transformation. The only difference under the  $H_1$  hypothesis is the conditional PDF of  $W$ . More precisely, conditioned on  $V$ ,  $W$  is the squared magnitude of a complex-Gaussian random variable with zero mean and variance  $\beta = \sigma^2 \mathbf{s}^H \Sigma^{-1} \mathbf{s} + v^2$ . Hence, the conditional probability of detection is given by  $P_{D|\Delta,V} = \int_{\sqrt{T^*}}^{\infty} \frac{1}{\beta} \exp(-\frac{r}{\beta}) dr = \exp(-\frac{T^*}{\beta})$ . The unconditional probability of detection is then obtained by using this expression in eq (1.15). Again, as in the previous case, closed-form evaluation of performance is not possible. The resulting integral must be calculated by using numerical methods. The Gaussian clutter case arises when  $h_{2JN}(x) = \exp(-x)$ . In this case,  $f_V(v) = \delta(v - 1)$ . Using these facts in eq (1.15), it follows that  $P_D = \exp(-\frac{T^*}{\beta})$  where  $\beta = \sigma^2 \mathbf{s}^H \Sigma^{-1} \mathbf{s} + 1$  and  $T^* = \ln(T)$ . As before, the data dependence of the threshold disappears.

Performance analysis is presented for the case of the K-distribution. The K-distributed envelope PDF, which is commonly used for modelling the amplitude statistics of land and sea clutter [19, 20], is a specific case of SIRPs. The in-phase and quadrature components of a K-distributed SIRV follow the generalized Laplace distribution. For this case, the

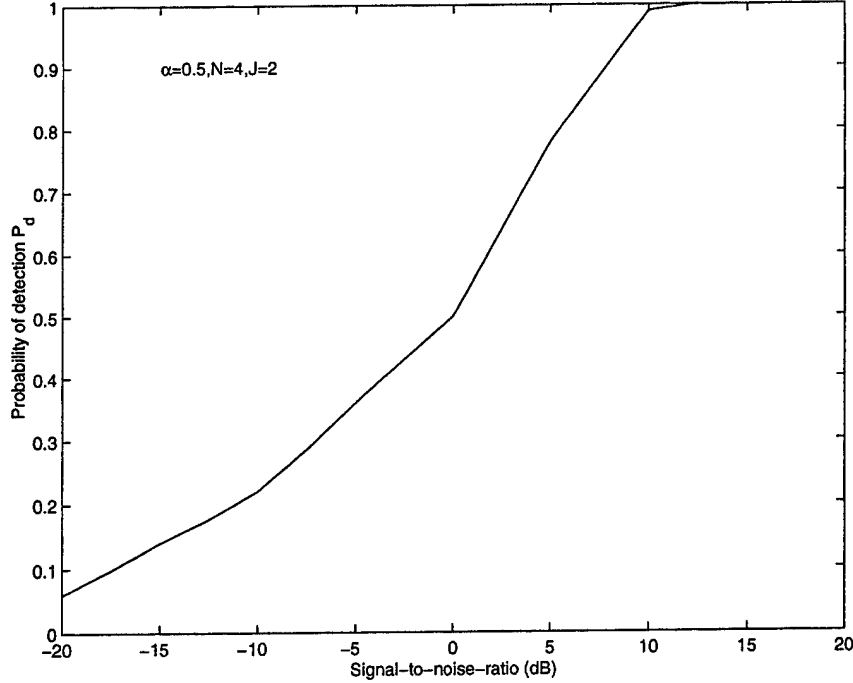


Figure 1.1: Probability of detection vs Signal-to-noise-ratio  $P_{fa} = 10^{-4}$

characteristic PDF and  $h_{2JN}(\cdot)$  are given by

$$\begin{aligned} f_V(v) &= \frac{2b}{\Gamma(\alpha)} (bv)^{2\alpha-1} \exp(-b^2v^2) u(v) \\ h_{2JN}(q) &= \frac{2b^{2JN}}{\Gamma(\alpha)} (b\sqrt{q})^{\alpha-JN} K_{\alpha-JN}(2b\sqrt{q}) \end{aligned} \quad (1.17)$$

where  $b$  is the scale parameter,  $\alpha$  is the shape parameter, and  $u(\cdot)$  is the unit step function. We use  $f_V(v)$  and  $h_{2JN}(\cdot)$  for the K-distribution in eq (1.12) to determine the threshold for a false alarm probability of  $10^{-4}$ . Detection probability is calculated using eq (1.15) by numerical integration. Probability of detection is plotted as a function of the signal-to-noise-ratio,  $|\hat{a}|^2 \mathbf{s}^H \Sigma^{-1} \mathbf{s}$ , for the case of  $\alpha = 0.5$  and  $\alpha = 0.1$  in Figures 1.1 and 1.2 respectively. Relevant test parameters are reported in the figures. In [21], the performance evaluation of the optimal receiver was carried out via Monte-Carlo simulations. The results of our analysis for the two test cases considered are in agreement with the results of [21].

## 1.4 Conclusions

We considered the performance of the optimal processor for target detection in additive non-Gaussian clutter which can be modeled as an SIRP. We derived integral expressions for the probability of false alarm and probability of detection for the case of a known signal with unknown complex amplitude. The results were then extended to the case of a signal with unknown complex amplitude following a complex-Gaussian distribution. The

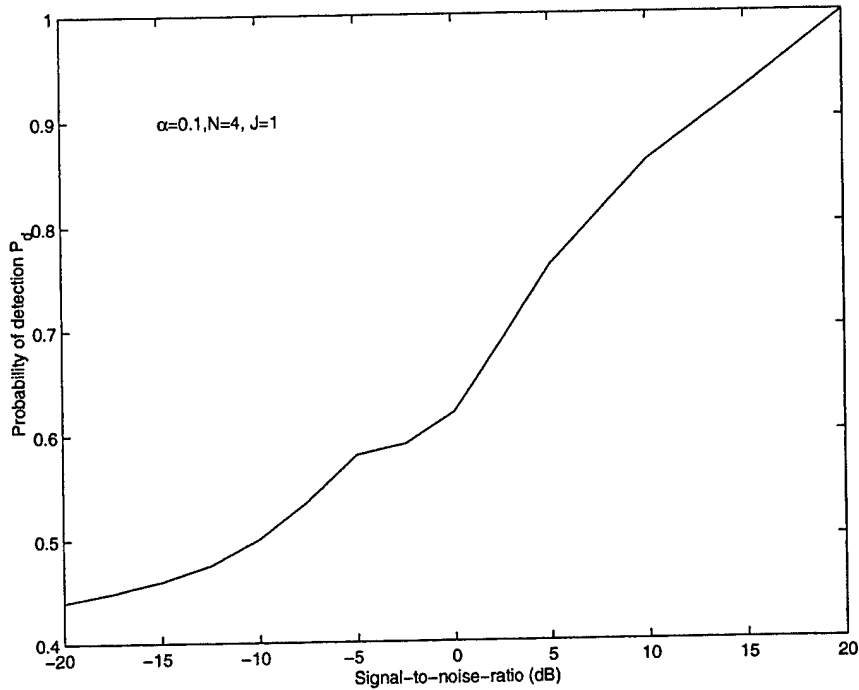


Figure 1.2: Probability of detection vs Signal-to-noise-ratio  $P_{fa} = 10^{-4}$

Householder transformation provided a useful technique for simplifying the analysis. As a result, several important properties of the Householder transformation have been documented in this work. Our results reduce to the well known expressions for the Gaussian matched filter as a special case. Except for the special case of Gaussian clutter, closed form or near closed form evaluation of the integrals is not possible. Further work needs to be undertaken to improve the numerical integration method used in this work.

## Chapter 2

# Analytical Expressions for the NMF and NAMF Tests

### 2.1 Test Statistic Descriptions

We now consider several non-adaptive and adaptive detection test statistics in this section.

#### 2.1.1 Non-Adaptive Test Statistics

The optimal receiver for detecting a rank one signal in Gaussian interference with known covariance matrix,  $\mathbf{R}_d$  is given by

$$\Lambda_{MF} = \frac{|\mathbf{e}^H \mathbf{R}_d^{-1} \mathbf{x}|^2}{\mathbf{e}^H \mathbf{R}_d^{-1} \mathbf{e}} \underset{H_0}{\overset{H_1}{>}} \lambda_{MF}. \quad (2.1)$$

In some instances, the test data vector is subject to an unknown scaling,  $\eta^2$ . Consequently, the test data covariance matrix takes the form  $\eta^2 \mathbf{R}_d$ . This corresponds to the scenario, where the covariance matrix has known structure but unknown level. The phase invariant matched filter (PI-MF) test for these problems is expressed as [22]

$$\Lambda_{PIMF} = \frac{|\mathbf{e}^H \mathbf{R}_d^{-1} \mathbf{x}|^2}{\eta^2 \mathbf{e}^H \mathbf{R}_d^{-1} \mathbf{e}} \underset{H_0}{\overset{H_1}{>}} \lambda_{PIMF} \quad (2.2)$$

where  $\mathbf{e}$  and  $\mathbf{x}$  are the concatenated  $JN \times 1$  signal ‘search’ steering and data vectors, respectively. The inner product of whitened vectors  $\mathbf{b} = \mathbf{R}_d^{-\frac{1}{2}} \mathbf{x}$  and  $\mathbf{f} = \mathbf{R}_d^{-\frac{1}{2}} \mathbf{e}$  is the matched filtering operation. Although (2.2) does not require knowledge of signal phase, it does require knowledge of the scale  $\eta$  to be CFAR. The normalized matched filter (NMF) test [14, 22–28] is given by

$$\Lambda_{NMF} = \frac{|\mathbf{e}^H \mathbf{R}_d^{-1} \mathbf{x}|^2}{[\mathbf{e}^H \mathbf{R}_d^{-1} \mathbf{e}][\mathbf{x}^H \mathbf{R}_d^{-1} \mathbf{x}]} \underset{H_0}{\overset{H_1}{>}} \lambda_{NMF}. \quad (2.3)$$

The whitening operation  $\mathbf{R}_d^{-\frac{1}{2}}$  transforms the signal and data vectors to obtain  $\mathbf{f}$  and  $\mathbf{b}$ , respectively. Consequently, the test statistic of (2.3) is simply the squared magnitude of the inner product of the vectors  $\mathbf{f}$  and  $\mathbf{b}$  normalized by their squared norms. Due to the Schwartz inequality,  $0 \leq \Lambda_{NMF} \leq 1$ .

### 2.1.2 Adaptive Test Statistics

For the adaptive problem,  $\hat{\mathbf{R}}_d$  replaces  $\mathbf{R}_d$  and the tests of (2.1) and (2.3) are referred to here as the AMF and NAMF, respectively. These tests are given by

$$\Lambda_{AMF} = \frac{|e^H \hat{\mathbf{R}}_d^{-1} \mathbf{x}|^2}{e^H \hat{\mathbf{R}}_d^{-1} \mathbf{e}} \underset{H_0}{\overset{H_1}{>}} \lambda_{AMF} \quad (2.4)$$

$$\Lambda_{NAMF} = \frac{|e^H \hat{\mathbf{R}}_d^{-1} \mathbf{x}|^2}{[e^H \hat{\mathbf{R}}_d^{-1} \mathbf{e}][\mathbf{x}^H \hat{\mathbf{R}}_d^{-1} \mathbf{x}]} \underset{H_0}{\overset{H_1}{>}} \lambda_{NAMF}. \quad (2.5)$$

Observe that  $\Lambda_{AMF}$  is simply the adaptive version of  $\Lambda_{MF}$  for the special case of  $\eta = 1$ . This result was developed independently in [7,15,29] where its CFAR behavior was noted. This property is lost when  $\eta \neq 1$ . Another important adaptive detection test known as the Kelly GLRT [6] is expressed as

$$\Lambda_{GLRT} = \frac{|e^H \hat{\mathbf{R}}_d^{-1} \mathbf{x}|^2}{[e^H \hat{\mathbf{R}}_d^{-1} \mathbf{e}][1 + \frac{\mathbf{x}^H \hat{\mathbf{R}}_d^{-1} \mathbf{x}}{K}]} \underset{H_0}{\overset{H_1}{>}} K \lambda_{GLRT} \quad (2.6)$$

where  $0 \leq \lambda_{GLRT} \leq 1$ . It is instructive to note that in the limit of large  $K$ , the tests of (2.4) and (2.6) converge to the test of (2.1), whereas the test of (2.5) converges to that of (2.3). It is instructive to note that in the limit of large  $K$ , the tests of (2.4) converges to the test of (2.1), whereas the test of (2.5) converges to that of (2.3).

The NAMF is invariant to changes in gain between training and test data and has been noted to be CFAR for the problem of Gaussian disturbance with a scale change between test and training data [22]; i.e., under  $H_1$ ,  $\mathbf{x} \sim CN(a\mathbf{e}, \eta^2 \mathbf{R}_d)$  while the training data  $\mathbf{z}$  collected under the  $H_0$  condition is considered to be complex-Gaussian distributed such that  $\mathbf{z} \sim CN(0, \mathbf{R}_d)$ . Thus, the variances of the training and test data differ by the factor  $\eta^2$ . In this chapter, we consider its performance in the more general problem involving the compound-Gaussian clutter model with power or scale changes over all range cells. No optimality claims of the NAMF test can be made for the case of SIRP disturbance.

## 2.2 Analytic Results

We present derivations of the false alarm and detection probabilities for the NMF test in SIRP clutter and the NAMF test for Gaussian clutter. Background white noise is not considered for tractability of analysis.

The test statistic of (2.3) can be expressed in terms of the whitened steering vector,  $\mathbf{f}$ , and the whitened test data vector,  $\mathbf{b}$  as

$$\Lambda_2 = \frac{|\mathbf{f}^H \mathbf{b}|^2}{[\mathbf{f}^H \mathbf{f}][\mathbf{b}^H \mathbf{b}]} \underset{H_0}{\overset{H_1}{>}} \lambda_2 \quad (2.7)$$

Noting that a unit vector in the direction of  $\mathbf{f}$  is given by  $\mathbf{f}_1 = \frac{\mathbf{f}}{(\mathbf{f}^H \mathbf{f})^{0.5}}$ ,  $\mathbf{b}^H \mathbf{b}$  can be expressed as the sum of the squared magnitudes of projections along the subspace of  $\mathbf{f}$  and the orthogonal complement space of  $\mathbf{f}$  denoted by  $\mathbf{P}_\perp$ . Let  $\mathbf{w}_i$ ,  $i = 1, 2, \dots, JN - 1$  denote an orthonormal basis set, for  $\mathbf{P}_\perp$  and  $X_0 = \mathbf{f}_1^H \mathbf{b}$ ,  $X_i = \mathbf{w}_i^H \mathbf{b}$ ,  $i = 1, 2, \dots, JN - 1$ . Then,  $X_i$ ,  $i = 0, 1, \dots, JN - 1$  are mutually uncorrelated univariate complex-SIRVs. Let  $\xi_1 = |X_0|^2$ ,  $\xi_2 = \sum_{i=1}^{JN-1} |X_i|^2$ , and  $\Phi = \frac{\xi_1}{\xi_2}$ . The test statistic of (2.7) admits a representation of the form

$$\Lambda_2 = \frac{\Phi}{(1 + \Phi)} \quad (2.8)$$

Under  $H_0$ ,  $X_i$ ,  $i = 0, 1, \dots, JN - 1$  are zero mean unit variance complex-SIRVs with characteristic PDF  $f_V(v)$ . Hence,  $X_i = Z_i V$ , where  $Z_i$ ,  $i = 0, 1, \dots, JN - 1$ , are iid CN(0,1) random variables. Let  $\chi_1 = |Z_0|^2$ ,  $\chi_{JN-1} = \sum_{i=1}^{JN-1} |Z_i|^2$ , and  $\Delta = \frac{\chi_1}{\chi_{JN-1}}$ . Thus, under  $H_0$ ,  $\Phi = \Delta$ . The test statistic of (2.7) reduces to

$$\Lambda_2 = \frac{\Delta}{(1 + \Delta)} \quad (2.9)$$

$\Delta$  is the ratio of two statistically independent Chi-Squared distributed random variables. Hence it follows the central-F distribution [30] given by

$$f_\Delta(\delta) = \frac{1}{\beta(JN - 1, 1)(1 + \delta)^{JN}} \quad (2.10)$$

where

$$\beta(m, n) = \int_0^1 \vartheta^{m-1} (1 - \vartheta)^{n-1} d\vartheta. \quad (2.11)$$

From (2.9) using a straightforward transformation of random variables, it follows that the PDF of  $\Lambda_2(\mathbf{x})$  under  $H_0$  is given by

$$f_{\Lambda_2}(r) = (JN - 1)(1 - r)^{JN-2}. \quad (2.12)$$

Consequently, the probability of false alarm is given by

$$P_{fa-NMF} = P(\Lambda_2 > \lambda_2 | H_0) = (1 - \lambda_2)^{JN-1}. \quad (2.13)$$

Under  $H_1$ , conditioned on  $V$ ,  $\xi_1$  is a non-central Chi-Square distributed random variable with noncentrality parameter  $A = |a|(\mathbf{e}^H \mathbf{R}_d^{-1} \mathbf{e})^{\frac{1}{2}}$  while  $\xi_2$  conditioned on  $V$  is a central chi-square distributed random variable with  $JN - 1$  degrees of freedom. Hence, conditioned

on  $V$ ,  $\Phi$  has a non-central F distribution. After some algebra, the PDF of  $\Lambda_2$  given  $V$  is expressed as

$$f_{\Lambda_2|V}(r|v) = \sum_{k=0}^{\infty} \exp\left(-\frac{A^2}{v^2}\right) \frac{A^{2k} r^k (1-r)^{JN-2}}{v^{2k} k! \beta(JN-1, k+1)} \quad 0 \leq r \leq 1 \quad (2.14)$$

The conditional probability of detection is given by

$$P_{d-NMF|V} = P[(\Lambda_2|V) > \lambda_2 | H_1] = \sum_{k=0}^{\infty} \exp\left(-\frac{A^2}{v^2}\right) \frac{A^{2k}}{v^{2k} k!} [1 - \text{betainc}(\lambda_2, k+1, JN-1)] \quad (2.15)$$

where

$$\text{betainc}(x, m, n) = \frac{1}{\beta(m, n)} \int_0^x \zeta^{m-1} (1-\zeta)^{n-1} d\zeta. \quad (2.16)$$

The unconditional probability of detection obtained by taking the expectation of (2.15) over  $V$  is given by

$$P_{d-NMF} = \sum_{k=0}^{\infty} h_{2k}(A^2) \frac{A^{2k}}{k!} [1 - \text{betainc}(\lambda_2, k+1, JN-1)] \quad (2.17)$$

where

$$h_{2k}(\psi) = \int_0^{\infty} v^{-2k} \exp\left(-\frac{\psi}{v^2}\right) f_V(v) dv. \quad (2.18)$$

Finite sum expressions for detection probabilities are reported in [31]. Using the results therein, the expression of (2.17) simplifies to

$$P_{d-NMF} = 1 - (1-\lambda_2)^{JN-1} \sum_{k=1}^{JN-1} \frac{\Gamma(JN)}{\Gamma(k+1)\Gamma(JN-k)} \left(\frac{\lambda_2}{1-\lambda_2}\right)^k g_k[A^2(1-\lambda_2)] \quad (2.19)$$

where

$$g_k(w) = \sum_{l=0}^{k-1} \frac{w^l}{\Gamma(l+1)} h_{2l}(w). \quad (2.20)$$

For the case of the K-distributed SIRP,

$$g_k(w) = \frac{2}{\Gamma(\alpha)} \sum_{l=0}^{k-1} \frac{\beta^{l+\alpha} w^{0.5\alpha+0.5l}}{\Gamma(l+1)} K_{\alpha-l}(2\beta\sqrt{w}) \quad (2.21)$$

For convenience, we set  $\beta = \sqrt{\alpha}$  in the examples presented. This normalization ensures unit mean square value for the modulating random variable  $V$ . The result of (2.19) is used in the examples presented in the next section. For the special case where  $h_{2l}(w) = \exp(-w)$ , (corresponding to Gaussian clutter), the expression of (2.19) reduces to

$$P_{d-NMF} = 1 - (1-\lambda_2)^{JN-1} \sum_{k=1}^{JN-1} \frac{\Gamma(JN)}{\Gamma(k+1)\Gamma(JN-k)} \left(\frac{\lambda_2}{1-\lambda_2}\right)^k [1 - \text{gammainc}(A^2(1-\lambda_2), k)] \quad (2.22)$$

where

$$\text{gammainc}(p, m) = \frac{1}{\Gamma(m)} \int_0^p \theta^{m-1} \exp(-\theta) d\theta \quad (2.23)$$

is the incomplete Gamma function.

We now consider the problem of performance evaluation of the NAMF in Gaussian clutter. The NAMF test statistic,  $\Lambda_{NAMF}$  is related to the Kelly GLRT test statistic,  $\Lambda_{GLRT}$  of (2.6) where  $\Gamma = \frac{1}{[1 + \mathbf{x}^H \hat{\mathbf{R}}_d^{-1} \mathbf{x} / K]}$  is the well known loss-factor with PDF [5]

$$f_{\Gamma}(\gamma) = \frac{1}{\beta(L+1, JN-1)} \gamma^L (1-\gamma)^{JN-2} \quad (2.24)$$

where  $L = K - JN + 1$ . Noting that  $\Lambda_{NAMF} = \frac{\Lambda_{GLRT}}{K(1-\Gamma)}$ , it follows from [6] that the probability of false alarm conditioned on  $\Gamma$  is given by

$$P_{fa-NAMF}|\Gamma = \frac{1}{[1 + (1-\gamma)\eta]^L} \quad (2.25)$$

where  $\eta$  is the threshold. The unconditional probability of false alarm is obtained by taking the expectation of (2.25) over  $\Gamma$  and is given by

$$P_{fa-NAMF} = \int_0^1 \frac{f_{\Gamma}(\gamma)}{[1 + (1-\gamma)\eta]^L} d\gamma. \quad (2.26)$$

Similarly from [6] the NAMF probability of detection conditioned on  $\Gamma$  is given by

$$P_{d-NAMF}|\Gamma = 1 - \frac{1}{[1 + (1-\gamma)\eta]^L} \sum_{m=1}^L \binom{L}{m} [\eta(1-\gamma)]^m [1 - \text{gammainc}\left(\frac{A(1-\gamma)}{1 + (1-\gamma)\eta}, m\right)]. \quad (2.27)$$

Taking the expectation of (2.27) over  $\Gamma$  yields the unconditional probability of detection, which is expressed as

$$P_{d-NAMF} = 1 - \int_0^1 \frac{1}{[1 + (1-\gamma)\eta]^L} \sum_{m=1}^L \binom{L}{m} [\eta(1-\gamma)]^m [1 - \text{gammainc}\left(\frac{A(1-\gamma)}{1 + (1-\gamma)\eta}, m\right)] f_{\Gamma}(\gamma) d\gamma. \quad (2.28)$$

For convenience,  $P_{d-NAMF}$  is expressed in terms of  $P_{dCFAR}$  of a scalar CFAR processor given by

$$P_{dCFAR}(\eta, A, L) = 1 - \frac{1}{(1+\eta)^L} \sum_{m=1}^L \binom{L}{m} \eta^m [1 - \text{gammainc}\left(\frac{A}{1+\eta}, m\right)]. \quad (2.29)$$

Numerical calculation of  $P_{d-NAMF}$  is obtained as

$$P_{d-NAMF} = \Delta\gamma \sum_{l=0}^{M-1} P_{dCFAR}[(1-l\Delta\gamma)\eta, (1-l\Delta\gamma)A, L] f_{\Gamma}(l\Delta\gamma) \quad (2.30)$$

where  $\Delta\gamma = \frac{1}{M}$ . Analytic expressions for the  $P_{fa}$  and  $P_d$  of the NAMF operating in Gaussian clutter were independently derived in [2,32]. The corresponding expressions for the NMF in compound-Gaussian clutter appear here for the first time.

In general, it is extremely difficult to derive the corresponding  $P_{fa}$  and  $P_d$  for the NAMF operating in SIRP clutter. This is due to the fact that the ML estimate of the SIRP covariance matrix is not available in closed form [33]. Hence, its PDF cannot be determined analytically. For the special case where the ML estimate of the SIRP clutter covariance matrix is to within a multiplicative constant of the sample covariance matrix [34], it is possible to derive the  $P_{fa}$  and  $P_d$  expressions for the NAMF in SIRP clutter. Specifically, for this scenario, the expression for  $P_{fa}$  remains unchanged from (2.26). However, the result for  $P_d$  is quite different from that of (2.28). The scenario where the ML estimate is to within a multiplicative constant of the sample covariance matrix corresponds to the case where the texture component of the SIRP is perfectly correlated. More precisely, for this scenario the texture component remains constant over all the training data realizations. However, real data seldom exhibits such a behavior [35]. Consequently,  $P_{fa}$  and  $P_d$  results for this scenario are merely of academic interest having little or no practical importance.

The  $P_{fa}$  and  $P_d$  expressions for the N-PAMF and PAMF operating in both Gaussian and non-Gaussian clutter scenarios are lacking since the analysis becomes mathematically intractable. Additionally, it is difficult to guarantee the CFAR behavior of the N-PAMF and PAMF with respect to the unknown covariance matrix. Consequently, performance evaluation of these methods is carried out by Monte-Carlo techniques. Performance results are presented in the next section.

## 2.3 Performance Results

Performance is now presented for the detectors described above. Figure 2.1 depicts the performance of the NMF in terms of  $P_d$  versus SINR in K-distributed SIRP for several shape parameter values. Relevant test parameters are provided in the plot. The  $P_d$  curves shown in this figure are obtained by using (2.19) and (2.22). It is instructive to observe the potential for improved NMF performance in impulsive clutter ( $\alpha = 0.1$ ). Furthermore, the NMF performance represents the upper bound on the performance of the N-PAMF and PAMF.

Figure 2.2 plots the NMF threshold as a function of the clutter shape parameter. Observe that the threshold is independent of the clutter shape parameter. Hence, the NMF is texture CFAR. This property is of considerable importance in practice, where estimation of the clutter shape parameter imposes onerous requirements of training data support. However, this property of the NMF is lost when the covariance matrix underlying the clutter is unknown. Specifically, it is shown in [36] that while operating SIRP clutter the NAMF employing a sample covariance matrix estimate incurs a considerable increase in the false alarm probability for small values of the shape parameter.

Figure 2.3 shows the performance of the NAMF operating in Gaussian clutter. Also

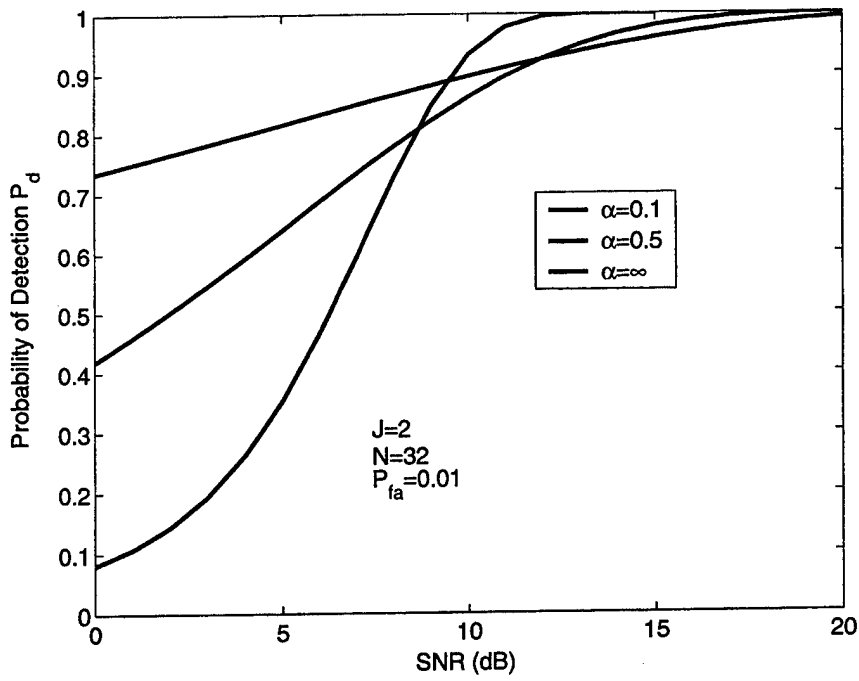


Figure 2.1: NMF performance in K-distributed SIRP disturbance

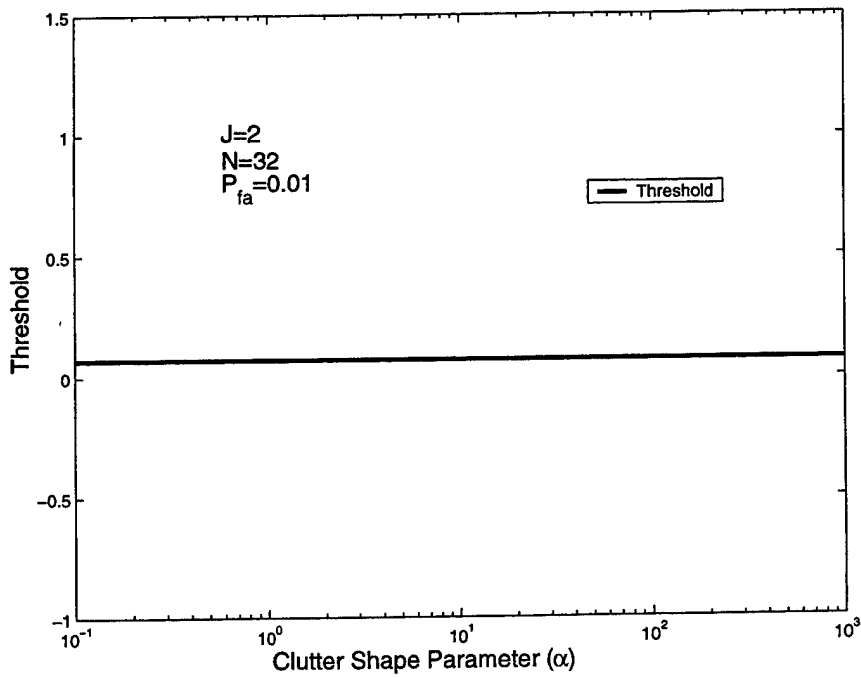


Figure 2.2: Threshold versus Shape Parameter

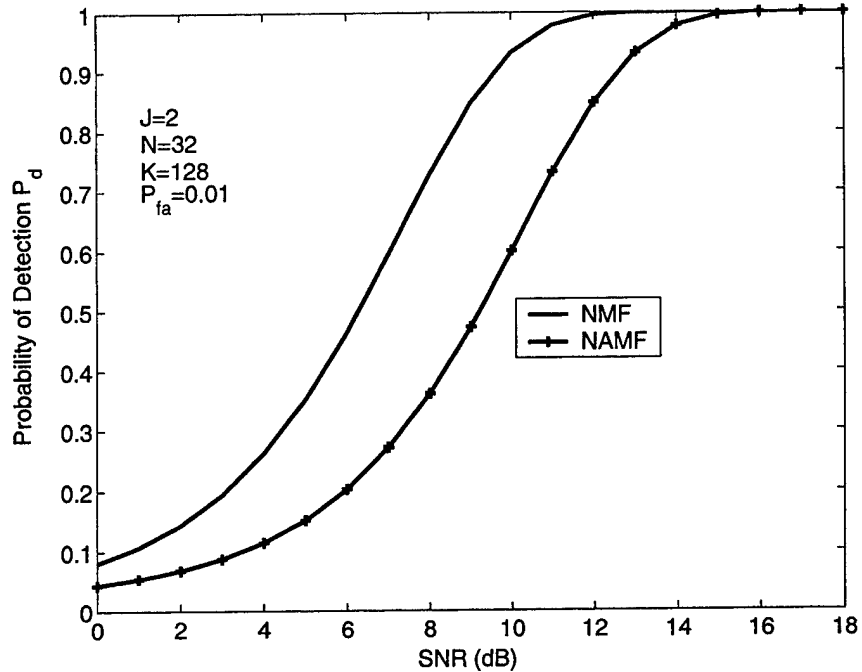


Figure 2.3: NMF Performance in Gaussian Clutter

shown is the performance of the NMF in Gaussian clutter. We observe that with  $K=2JN$ , for a given probability of detection, the SNR required by the NAMF is approximately 3 dB larger than the corresponding SNR for the NMF.

Figure 2.4 presents a performance comparison of the NAMF, AMF and Kelly GLRT in Gaussian clutter. For the example presented, the Kelly GLRT performs slightly better than the NAMF and CFAR-AMF. The latter two methods have comparable performance.

## 2.4 Summary

In this chapter, we presented analytic expressions for the probability of detection and probability of false alarm for the NMF operating in compound-Gaussian clutter. The texture CFAR feature of the NMF was noted. Probability of detection and false alarm for the NAMF operating in Gaussian clutter is also presented. Performance of the NAMF is compared with that of the NMF operating in Gaussian clutter. Approximately 3dB difference in performance was noted for  $K=2JN$ .

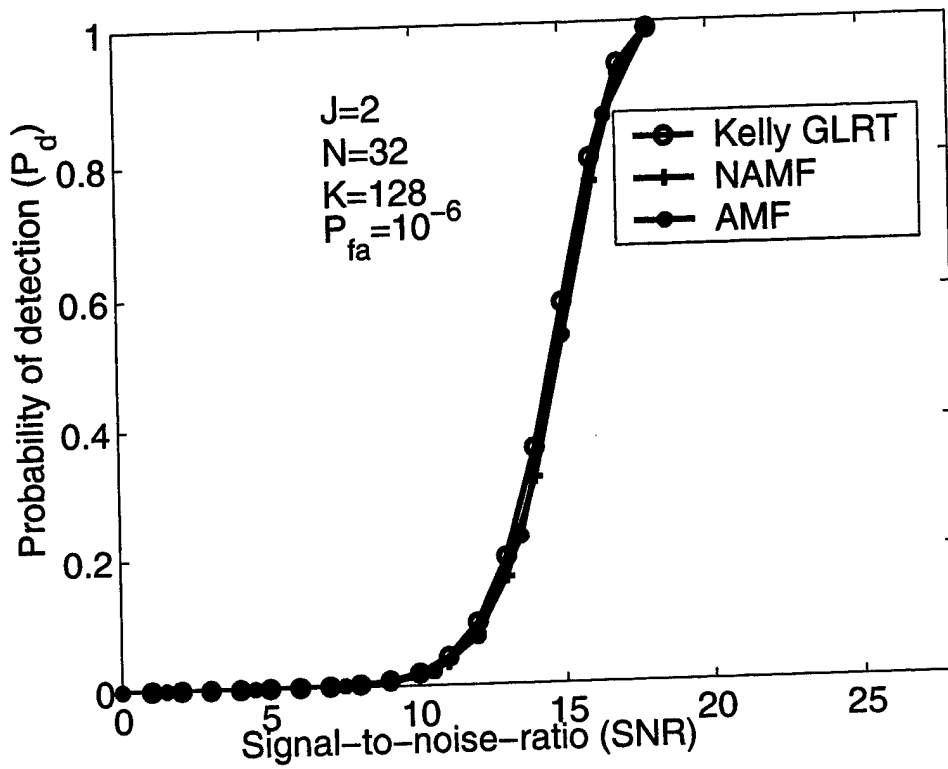


Figure 2.4: NAMF, Kelly GLRT, CFAR-AMF Performance in Gaussian Clutter

# Chapter 3

## Statistical Analysis of the Nonhomogeneity Detector

### 3.1 Introduction

An important issue in space-time adaptive processing (STAP) for radar target detection is the formation and inversion of the covariance matrix underlying the clutter/interference. In practice, the unknown interference covariance matrix is estimated from a set of independent identically distributed (iid) target-free training data which is assumed to be representative of the interference statistics in a cell under test. Frequently, the training data is subject to contamination by discrete scatterers or interfering targets. In either event, the training data becomes nonhomogeneous. As a result, it is non representative of the interference in the test cell. Estimates of the covariance matrix from nonhomogeneous training data result in severely undernulled clutter. Consequently, CFAR and detection performance suffer. Significant performance improvement can be achieved by employing pre-processing to select representative training data.

The problem of target detection using improved training strategies has been considered in [37–44]. The impact of nonhomogeneity on STAP performance is considered in [44–47]. The works of [37–40,44,48] have addressed the use of the non-homogeneity detector (NHD) based on the generalized inner product (GIP) measure for STAP problems. The GIP is used as a measure to select representative training data by the NHD. In this chapter, we provide a statistical analysis of the GIP based NHD for Gaussian interference statistics.

### 3.2 GIP Statistics: Known Covariance

Let  $\mathbf{x} = [x_1 \ x_2 \ \dots \ x_M]^T$  denote a complex random vector with zero mean and known positive definite Hermitian covariance matrix  $\mathbf{R}$ . The quadratic form given by  $Q = \mathbf{x}^H \mathbf{R}^{-1} \mathbf{x}$  has the important property that  $E(Q) = M$  [30]. This result is readily proven below.

$$Q = \mathbf{x}^H \mathbf{R}^{-1} \mathbf{x} = \text{tr}[\mathbf{x}^H \mathbf{R}^{-1} \mathbf{x}] = \text{tr}[\mathbf{R}^{-1} \mathbf{x} \mathbf{x}^H] \quad (3.1)$$

where  $tr(\cdot)$  denotes the trace of a matrix. We have made use of the fact that  $tr(\mathbf{AB}) = tr(\mathbf{BA})$ . Hence,

$$\begin{aligned} E(Q) &= E\{tr[\mathbf{R}^{-1}\mathbf{x}\mathbf{x}^H]\} = tr[\mathbf{R}^{-1}E\{\mathbf{x}\mathbf{x}^H\}] \\ &= tr(\mathbf{R}^{-1}\mathbf{R}) = tr(\mathbf{I}_M) = M \end{aligned} \quad (3.2)$$

where  $\mathbf{I}_M$  is the  $M \times M$  identity matrix. This result is important in that it is independent of the PDF underlying  $\mathbf{x}$  and is only a function of the dimension of the random vector.

If the PDF of  $\mathbf{x}$  is known, the corresponding PDF of  $Q$  can be readily derived. For Gaussian distributed  $\mathbf{x}$ , i.e.,  $\mathbf{x} \sim CN(0, \mathbf{R})$ , the PDF of  $Q$  is a Chi-Squared distribution with  $M$  complex degrees of freedom. More precisely,

$$Q = \mathbf{x}^H \mathbf{R}^{-1} \mathbf{x} = \|\mathbf{R}^{-\frac{1}{2}} \mathbf{x}\|^2 \quad (3.3)$$

where  $\|\cdot\|$  denotes the Euclidean vector norm. Letting  $\mathbf{y} = \mathbf{R}^{-\frac{1}{2}} \mathbf{x}$  gives

$$Q = \|\mathbf{y}\|^2 = \sum_{i=1}^M |Y_i|^2 \quad (3.4)$$

where  $Y_i$ ,  $i = 1, 2, \dots, M$  are iid  $CN(0, 1)$  random variables. Since  $Q$  is the sum of the squared magnitudes of  $M$  iid  $CN(0, 1)$  random variables, it follows that  $Q$  is a Chi-Squared distributed random variable with  $M$  complex degrees of freedom [30]. The PDF of  $Q$  is given by

$$f_Q(q) = \frac{q^{M-1}}{\Gamma(M)} \exp(-q) \quad 0 \leq q < \infty \quad (3.5)$$

where  $\Gamma(\cdot)$  is the Euler-Gamma function.

The GIP based NHD calculates the quadratic form  $Q$  using an estimated covariance matrix (formed from iid target free training data) and compares its mean with the dimensionality of the random vector  $\mathbf{x}$ . Deviations from  $M$  have been attributed to non-homogeneities in the training data [37–40, 44]. In practice, the interference covariance matrix is formed from a finite amount of training data. The statistical variability associated with the data could introduce additional errors and thus deviations of the GIP from  $M$  cannot entirely be ascribed to the presence of non-homogeneities. Consequently, it is useful to work with the statistics of  $Q$  formed with an estimated covariance matrix.

### 3.3 GIP Statistics: Unknown Covariance

The complex-Gaussian test data vector is denoted by  $\mathbf{x} \sim CN(0, \mathbf{R}_T)$ , where  $\mathbf{R}_T$  is unknown. Let  $\mathbf{z}_i$ ,  $i = 1, 2, \dots, K$  denote iid  $CN(0, \mathbf{R}_z)$  target free training data. For representative (homogeneous) training data,  $\mathbf{R}_T = \mathbf{R}_z = \mathbf{R}$ . The maximum likelihood estimate of the covariance matrix is given by

$$\hat{\mathbf{R}} = \frac{1}{K} \sum_{i=1}^K \mathbf{z}_i \mathbf{z}_i^H. \quad (3.6)$$

Let  $P = \mathbf{x}^H \hat{\mathbf{R}}^{-1} \mathbf{x}$ . A stochastic representation for the normalized GIP denoted by  $P' = \frac{P}{K}$  is derived in appendix A. Consequently,  $P$  can be expressed as

$$P = \frac{KR_1}{R_2} \quad (3.7)$$

where  $R_1$  and  $R_2$  are statistically independent Chi-squared distributed random variables with PDFs given by

$$f_{R_1}(r_1) = \frac{r_1^{M-1}}{\Gamma(M)} \exp(-r_1) \quad 0 \leq r_1 < \infty \quad (3.8)$$

$$f_{R_2}(r_2) = \frac{r_2^{K-M}}{\Gamma(K-M+1)} \exp(-r_2) \quad 0 \leq r_2 < \infty \quad (3.9)$$

respectively. The PDF of  $P'$ , which is simply a central-F distribution [49], is expressed as

$$f_{P'}(r) = \frac{1}{\beta(L, M)} \frac{r^{M-1}}{(1+r)^{M+L}} \quad 0 \leq r < \infty \quad (3.10)$$

where  $L = K - M + 1$  and

$$\beta(m, n) = \int_0^1 \theta^{m-1} (1-\theta)^{n-1} d\theta. \quad (3.11)$$

The statistical equivalence of  $P$  to within a scalar of the ratio of two independent chi-square distributed random variables is fascinating in that it permits rapid calculation of the moments of  $P$ . More importantly, it is extremely useful in Monte-Carlo studies involving computer generation of  $P$ . For homogeneous training data, the use of (3.7) circumvents the need to explicitly generate the test data vector  $\mathbf{x}$  and the training data vectors used for covariance estimation. For large  $M$  and perforce  $K$ , significant computational savings can be realized from the method of (3.7).

It can be readily shown that

$$E(P) = KE(R_1)E(R_2^{-1}) = \frac{M}{[1 - \frac{M}{K}]} \quad (3.12)$$

$$\sigma_P^2 = \frac{M}{[1 - \frac{M}{K}][1 - \frac{(M+1)}{K}]}$$

where  $E(P)$  and  $\sigma_P^2$  denote the mean and variance of  $P$ , respectively. We then consider the PDF of  $\frac{R_2}{K}$  in the limit of large  $K$ . The characteristic function of  $\frac{R_2}{K}$  is given by

$$\Phi_{R_2}(j\omega) = E[\exp(-j\omega \frac{R_2}{K})] = \frac{1}{(1 + \frac{j\omega}{K})^{K-M+1}}. \quad (3.13)$$

In the limit of  $K \rightarrow \infty$ , we have

$$\Psi(j\omega) = \lim_{K \rightarrow \infty} \Phi_{R_2}(j\omega) = \exp(-j\omega). \quad (3.14)$$

The PDF of  $\frac{R_2}{K}$  in the limit of  $K \rightarrow \infty$  is given by

$$f_{R_2}(r) = \frac{1}{2\pi} \int_{-\infty}^{\infty} \exp[(r-1)j\omega] d\omega = \delta(r-1). \quad (3.15)$$

Hence, for  $K \rightarrow \infty$ ,  $R_2/K$  becomes unity with probability 1. Consequently, the GIP is simply  $R_1$  and hence, follows a Chi-Squared distribution with  $M$  complex degrees of freedom. Thus for  $K \rightarrow \infty$ ,  $E(P) = M$  and  $\sigma_P^2 = M$ , corresponding to the known covariance matrix results. Consequently, the GIP statistical representation given by (3.7) provides additional insights into the NHD. The numerator random variable corresponds to the GIP statistics for known covariance matrix. The denominator random variable succinctly embeds the deleterious effects of estimating the covariance matrix with finite sample support as well as nonhomogeneity of the training data. A manifestation of this effect can be seen from the deviation of the statistics of  $R_2$  from the Chi-Squared distribution.

### 3.4 New Test for Nonhomogeneity

The work of [37-40,44] uses an NHD based on comparing the mean of empirically formed GIPs (from different realizations of test data) to  $M$ . Large deviations from  $M$  are ascribed to nonhomogeneities. However, the effects of finite data support and the associated statistical variability can result in large deviations of the empirical GIP mean from  $M$ . Thus, a more stringent test for the GIP based NHD consists of the following steps:

1. Form the GIP denoted by  $P$  for a given  $K$ .
2. Perform a goodness-of-fit test of the empirically formed  $\frac{P}{K}$  with the theoretically predicted PDF of (3.10). Specifically, we set the type-I error,  $\alpha$ , to be 0.1. This is simply the probability of incorrectly rejecting the hypothesis that the data comes from the F-distribution of (3.10). More precisely, this corresponds to calculating a threshold  $\lambda$ , such that  $\alpha = Pr(P' > \lambda) = 0.1$ . From (3.10), it follows that

$$Pr(P' > \lambda) = \text{betainc}\left(\frac{1}{\lambda+1}, M, L\right) \quad (3.16)$$

where

$$\text{betainc}(x, M, L) = \frac{1}{\beta(M, L)} \int_0^x \theta^{M-1} (1-\theta)^{L-1} d\theta. \quad (3.17)$$

Given  $\alpha$ ,  $M$ , and  $L$ ,  $\lambda$  is readily calculated from an inversion of (3.16). The goodness-of-fit test consists of comparing the empirically formed  $P'$  from each training data realization with  $\lambda$  and rejecting those realizations for which  $P'$  exceeds  $\lambda$ .

3. Compare the empirical GIP mean to the theoretically predicted mean value of (3.12). Large discrepancies between the theoretical and empirical means result from non-homogeneities. This serves as an independent validation of step 2.
4. Histogram plots of the empirical values of  $\frac{P}{K}$  overlaid on the theoretical PDF of  $P'$  serve as an additional check on the results of steps 2 and 3.

### 3.5 Performance Analysis

We present performance results of our approach here. Figure 3.1 shows the PDF of  $P'$  for several values of  $K$  with  $M=8$  for Gaussian interference statistics. Observe that the variance of  $P'$  decreases with increasing  $K$ . This is anticipated since  $\hat{\mathbf{R}}$  tends to  $\mathbf{R}$  with probability 1 as  $K \rightarrow \infty$ . The results presented in Figures 3.2 and 3.3 correspond to the case of homogeneous training data. Figure 3.2 presents a comparison of the cumulative distribution function (CDF) of  $P'$  obtained from Monte-Carlo realizations using simulated data with the theoretically predicted CDF of  $P'$  obtained by numerical integration of (3.10). Figure 3.3 plots the theoretical PDF of  $P'$  given by (3.10) over the histogram obtained from Monte-Carlo data for  $M=8$  and  $K=16$ . The results show good agreement between the theoretical prediction and the empirically generated values. The mean value of  $P$ , 15.957, obtained via Monte-Carlo compares well with the theoretically predicted value of 16. Figure 3.4 plots the type-I error versus threshold for  $M=64$ . Here different values of  $K$  are chosen to illustrate the threshold behavior. For each value of  $\alpha$ ,  $\lambda$  is determined from a numerical inversion of (3.16). For a given  $\alpha$  we observe an increase in  $\lambda$  with increasing  $K$ . Figure 3.5 shows the results of the goodness of fit test for the MCARM data [50] using acquisition '220' on Flight 5, cycle 'e' for 8 channels and 16 pulses. The normalized GIP and the threshold are plotted as a function of range. Non-homogeneity of the training data is evident in those bins for which the normalized GIP exceeds the threshold.

### 3.6 Conclusion

This work extends the results of previous work on non-homogeneity detection by providing a rigorous statistical characterization of the NHD for Gaussian interference. It is shown that the NHD statistic admits a simple representation as a ratio of two statistically independent Chi-squared distributed random variables. A formal goodness-of-fit test based on this representation, which follows an F-distribution, is derived. Performance analysis of the method is considered in some detail. The illustrative examples validate the approach taken and confirm the results. Future work would include extensive performance analysis using simulated and measured data showing the resulting impact on STAP performance. The performance of several STAP algorithms in Gaussian and non-Gaussian interference scenarios has been considered in [36]. Future work will address performance of the methods treated in [36] with suitable NHD pre-processing.

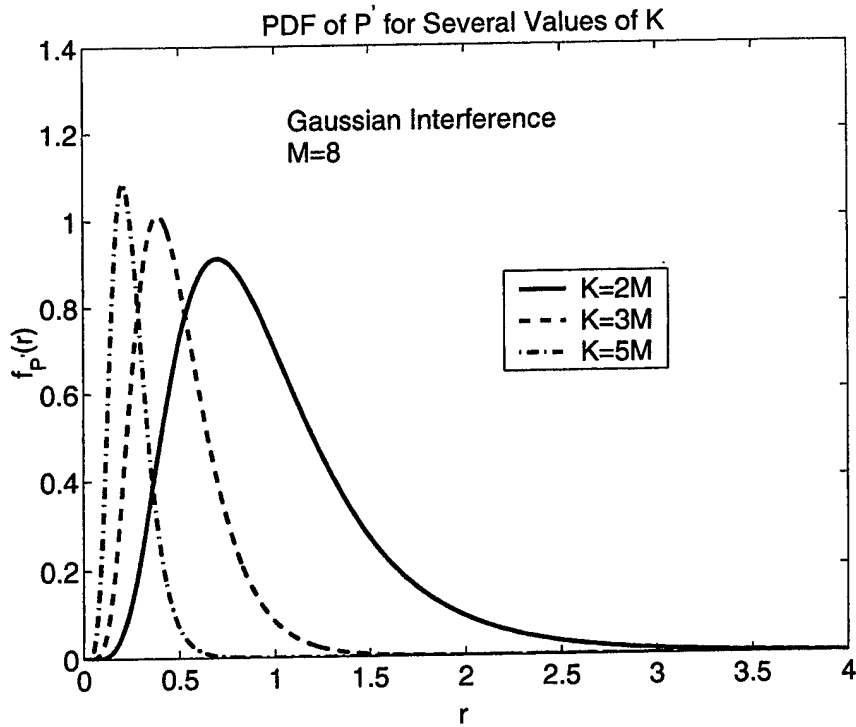


Figure 3.1: PDF of the normalized GIP

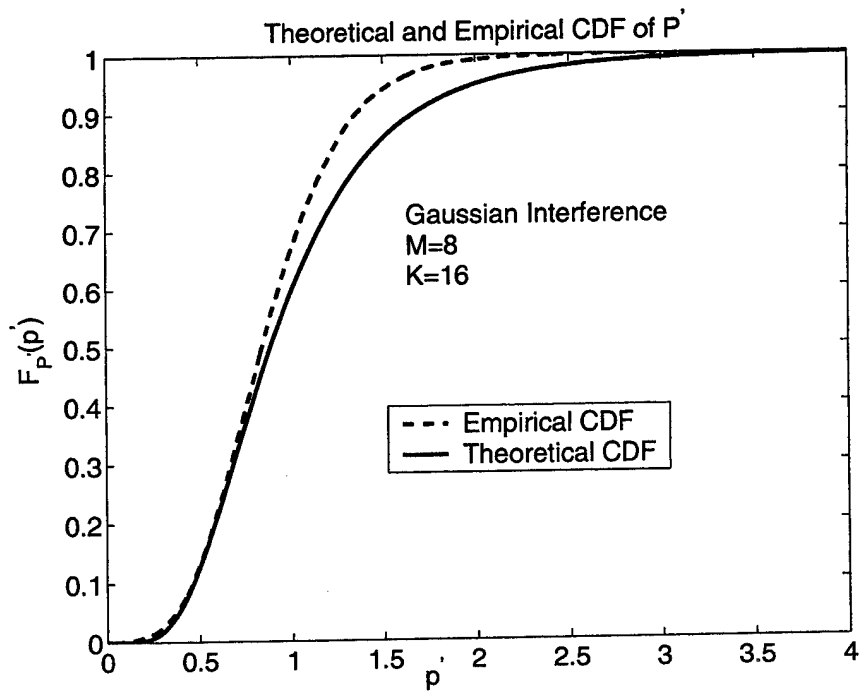


Figure 3.2: Theoretical and empirical CDF of the normalized GIP

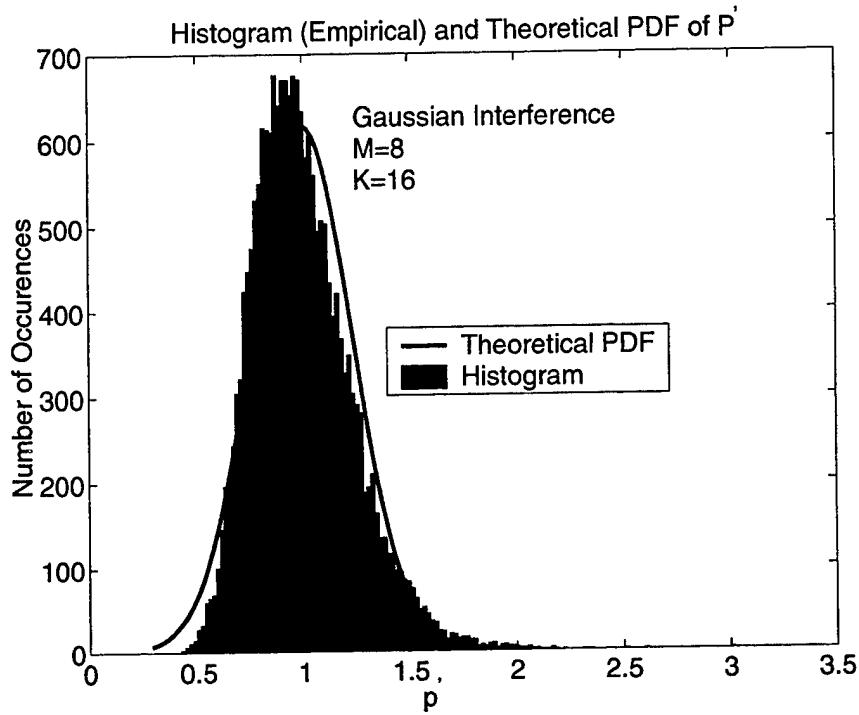


Figure 3.3: Histogram of empirical data and theoretical PDF of the normalized GIP

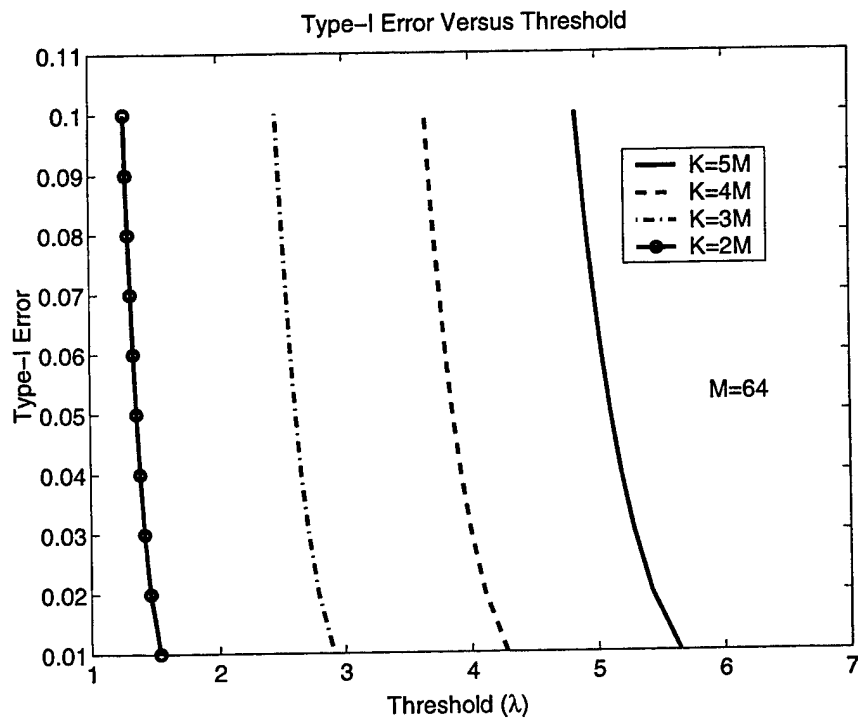


Figure 3.4: Type-I error versus threshold

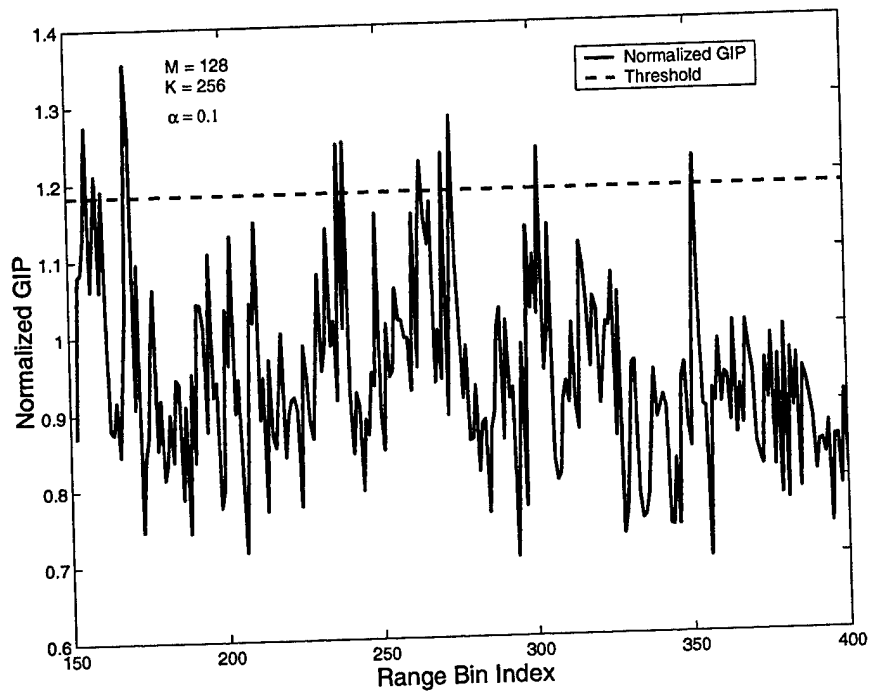


Figure 3.5: Normalized GIP vs Range

# Bibliography

- [1] M. Rangaswamy and J. H. Michels, "Performance Analysis of Space-Time Adaptive Processing Methods in Non-Gaussian Radar Clutter Backgrounds," in *Proceedings of the International Conference on Radar Systems*, (Brest, France), 1999.
- [2] J. Michels, M. Rangaswamy, and B. Himed, "Performance of STAP tests in compound Gaussian clutter," in *Proceedings of the First IEEE Workshop on Sensor Array and Multichannel Processing (SAM-2000)*, (Cambridge, MA), 2000.
- [3] M. Rangaswamy, B. Himed, and J. Michels, "Statistical analysis of the nonhomogeneity detector," in *Proceedings of the 34th Asilomar Conference on Signals, Systems, and Computers*, (Pacific Grove, CA), 2000.
- [4] L. E. Brennan and I. S. Reed, "Theory of adaptive radar," *IEEE Trans. on Aerospace and Electronic Systems*, vol. **AES-9**, pp. 237–252, 1973.
- [5] I. Reed, J. Mallett, and L. Brennan, "Rapid convergence rate in adaptive arrays," *IEEE Trans. on Aerospace and Electronic Systems*, vol. **AES-10**, pp. 853–863, 1974.
- [6] E. Kelly, "An adaptive detection algorithm," *IEEE Trans. on Aerospace and Electronic Systems*, vol. **AES-22**, pp. 115–127, 1986.
- [7] F. Robey, D. Fuhrmann, E. Kelly, and R. Nitzberg, "A CFAR adaptive matched filter detector," *IEEE Trans. on Aerospace and Electronic Systems*, vol. **AES-28**, pp. 208–216, 1992.
- [8] S. Haykin and A. Steinhardt, *Adaptive Radar Detection and Estimation*. New York: John Wiley and sons, 1992.
- [9] M. Rangaswamy, J. Michels, and D. Weiner, "Multichannel detection for correlated non-Gaussian random processes based on innovations," *IEEE Trans. on Signal Processing*, vol. **SP-43**, pp. 1915–1922, 1995.
- [10] M. Rangaswamy and J. Michels, "A Parametric Multichannel Detection Algorithm For Correlated Non-Gaussian Random Processes," in *Proceedings of the IEEE National Radar Conference*, (Syracuse, NY), 1997.

- [11] M. Rangaswamy and J. Michels, "A Parametric Detection Algorithm for Space-Time Adaptive Processing in Non-Gaussian Radar Clutter Backgrounds," *Signal Processing*, 2001 (to appear).
- [12] J. Michels, T. Tsao, B. Himed, and M. Rangaswamy, "Space-Time Adaptive Processing (STAP) in Airborne Radar Applications," in *Proceedings of the IASTED Conference on Signal Processing and Communications*, (Canary Islands, Spain), 1998.
- [13] F. Gini, M. Greco, and L. Verrazzani, "Detection problem in mixed clutter environment as a Gaussian problem by adaptive pre-processing," *Electronic Letters*, vol. 31, No.14, pp. 1189-1190, 1995.
- [14] F. Gini, "Sub-optimum coherent radar detection in a mixture of K-distributed and Gaussian clutter," *IEE Proc.F, Radar, Sonar and Navigation*, vol. 144 (1), pp. 39-48, 1997.
- [15] L. Cai and H. Wang, "On adaptive filtering with the CFAR feature and its performance sensitivity to non-Gaussian interference," in *Proceedings of the 24th Annual conference on Information Sciences and Systems*, (Princeton, NJ), pp. 558-563, 1990.
- [16] M. Rangaswamy, D. Weiner, and A. Ozturk, "Non-Gaussian random vector identification using spherically invariant random processes," *IEEE Trans. on Aerospace and Electronic Systems*, vol. AES-29, pp. 111-124, 1993.
- [17] S. Haykin, *Adaptive Filter Theory*. New Jersey: Prentice Hall, 1996.
- [18] K. Yao, "A representation theorem and its applications to spherically invariant random processes," *IEEE Trans. on Information Theory*, vol. IT-19, pp. 600-608, 1973.
- [19] J. Jao, "Amplitude distribution of composite terrain radar clutter and the K-distribution," *IEEE Trans. on Antennas and Propagation*, vol. AP-32, pp. 1049-1062, 1984.
- [20] E. Jakeman and P. Pusey, "A model for non-Rayleigh sea echo," *IEEE Trans. on Antennas and Propagation*, vol. AP-24, pp. 806-814, 1976.
- [21] E. Conte, M. Longo, M. Lops, and S. Ullo, "Radar detection of signals with unknown parameters in K-distributed clutter," *IEE Proc.F, Radar, Sonar and Navigation*, vol. 138, (2), pp. 131-138, 1991.
- [22] S. Kraut, T. McWhorter, and L. Scharf, "A canonical representation for the distributions of adaptive matched subspace detectors," in *Proceedings of the 31th Asilomar Conference on Signals, Systems, and Computers*, (Pacific Grove, CA), 1997.
- [23] E. Conte, M. Lops, and G. Ricci, "Asymptotically optimum radar detection in compound-Gaussian clutter," *IEEE Trans. on Aerospace and Electronic Systems*, vol. AES-31, pp. 617-625, 1995.

- [24] L. Scharf, *Statistical Signal Processing*. Reading, MA: Addison-Wesley Publishing Company, 1990.
- [25] L. Scharf and B. Friedlander, "Matched Subspace Detectors," *IEEE Trans. on Signal Processing*, vol. **SP-42**, pp. 2146–2157, 1994.
- [26] L. Scharf and T. McWhorter, "Adaptive Matched Subspace Detector and Adaptive Coherence Estimators," in *Proceedings of the 30th Asilomar Conference on Signals, Systems, and Computers*, (Pacific Grove, CA), 1996.
- [27] L. Scharf, T. McWhorter, and L. Griffiths, "Adaptive Coherence Estimation for Radar Signal Processing," in *Proceedings of the 30th Asilomar Conference on Signals, Systems, and Computers*, (Pacific Grove, CA), 1996.
- [28] S. Kraut and L. Scharf, "The CFAR Adaptive Subspace Detector is a Scale-Invariant GLRT," *IEEE Trans. on Signal Processing*, vol. **SP-47**, pp. 2538–2541, 1999.
- [29] W. Chen and I. Reed, "A new CFAR detection test for radar," *Digital Signal Processing*, vol. **1**, pp. 198–214, 1991.
- [30] A. Papoulis, *Probability, Random Variables and Stochastic Processes*. New York: McGraw-Hill, 1991.
- [31] E. Kelly, "Finite Sum expressions for signal detection probabilities," Tech. Rep. 566, " MIT Lincoln Laboratory, May 1981.
- [32] C. Richmond, "Performance of the adaptive sidelobe blanker detection algorithm in homogeneous environments," *IEEE Trans. on Signal Processing*, vol. **SP-48**, no. 5, pp. 1235–1247, 2000.
- [33] M. Rangaswamy and J. H. Michels, "Adaptive Processing in Non-Gaussian Noise Backgrounds," in *Proceedings of the Ninth IEEE Workshop on Statistical Signal and Array Processing*, (Portland, OR), 1998.
- [34] K. Fang and T. Anderson, *Statistical Inference in Elliptically Contoured and Related Distributions*. New York: Allerton Press inc., 1990.
- [35] F. Gini and J. Michels, "Performance analysis of two covariance matrix estimators in compound Gaussian clutter," *IEE Proc.F, Radar, Sonar and Navigation*, vol. **146**, (3), 1999.
- [36] J. Michels, B. Himed, and M. Rangaswamy, "Performance of STAP tests in Gaussian and Compound-Gaussian Clutter," *Digital Signal Processing*, vol. **10**, no. 4, pp. 309–324, 2000.
- [37] P. Chen, "On testing the equality of covariance matrices under singularity," tech. rep., for AFOSR Summer Faculty Research Program, Rome Laboratory, August 1994.

- [38] P. Chen, "Partitioning procedure in radar signal processing problems," tech. rep., for AFOSR Summer Faculty Research Program, Rome Laboratory, August 1995.
- [39] W. Melvin, M. Wicks, and R. Brown, "Assessment of multichannel airborne radar measurements for analysis and design of space-time adaptive processing architectures and algorithms," in *Proceedings of the IEEE National Radar Conference*, (Ann Arbor, MI), 1996.
- [40] W. Melvin and M. Wicks, "Improving practical space-time adaptive radar," in *Proceedings of the IEEE National Radar Conference*, (Syracuse, NY), 1997.
- [41] D. Rabideau and A. Steinhardt, "Improving the performance of adaptive arrays in nonstationary environments through data-adaptive training," in *Proceedings of the 30th Asilomar Conference on Signals, Systems, and Computers*, (Pacific Grove, CA), 1996.
- [42] D. Rabideau and A. Steinhardt, "Power selected training for false alarm mitigation in airborne radar," in *Proceedings of the Adaptive Sensor Array Processing Workshop (ASAP)*, (MIT Lincoln Laboratory, Lexington, MA), 1996.
- [43] D. Rabideau and A. Steinhardt, "Improved adaptive clutter cancellation through data-adaptive training," *IEEE Trans. on Aerospace and Electronic Systems*, vol. **AES-35**, no.3, pp. 879-891, 1999.
- [44] B. Himed, Y. Salama, and J. H. Michels, "Improved detection of close proximity targets using two-step NHD," in *Proceedings of the International Radar Conference*, (Alexandria,VA), 2000.
- [45] R. Nitzberg, "An effect of range-heterogenous clutter on adaptive Doppler filters," *IEEE Trans. on Aerospace and Electronic Systems*, vol. **26**, no.3, pp. 475-480, 1990.
- [46] W. L. Melvin, J. R. Guerci, M. J. Callahan, and M. C. Wicks, "Design of adaptive detection algorithms for surveillance radar," in *Proceedings of the International Radar Conference*, (Alexandria,VA), 2000.
- [47] W. L. Melvin, "Space-time adaptive radar performance in heterogenous clutter," *IEEE Trans. on Aerospace and Electronic Systems*, vol. **36**, no.2, pp. 621-633, 2000.
- [48] P. Chen, W. Melvin, and M. Wicks, "Screening among multivariate normal data," *Journal of Multivariate Analysis*, vol. 69, pp. 10-29, 1999.
- [49] T. Anderson, *An introduction to multivariate statistical analysis*. New York: John Wiley and sons, 1958.
- [50] MCARMDATA, "View www@http://128.132.2.229." Data from the Multichannel Airborne Radar Measurement Program of the U.S. Air Force Research Laboratory, Rome, NY.

# Appendix A: Stochastic Representation for the Normalized GIP

Let  $\mathbf{Z}$  denote a data matrix whose columns are the previously defined  $\mathbf{z}_i$ ,  $i = 1, 2, \dots, K$ . The maximum likelihood estimate of the covariance matrix is then expressed as  $\hat{\mathbf{R}} = \frac{1}{K} \mathbf{S}_z$ , where  $\mathbf{S}_z = \mathbf{Z}\mathbf{Z}^H$ . Consequently, the normalized GIP is expressed as

$$P' = \mathbf{x}^H \mathbf{S}_z^{-1} \mathbf{x}. \quad (3.18)$$

The data matrix  $\mathbf{Z}$  and the vector  $\mathbf{x}$  admit a statistical representation of the form

$$\begin{aligned} \mathbf{Z} &= \mathbf{R}^{\frac{1}{2}} \mathbf{Y} \\ \mathbf{x} &= \mathbf{R}^{\frac{1}{2}} \mathbf{y} \end{aligned} \quad (3.19)$$

where  $\mathbf{Y}$  is a data matrix whose columns,  $\mathbf{y}_i$ ,  $i = 1, 2, \dots, K$  are iid  $\text{CN}(0, \mathbf{I})$  random vectors and  $\mathbf{y}$  is a  $\text{CN}(0, \mathbf{I})$  random vector, which is statistically independent of  $\mathbf{Y}$ . Hence, the normalized GIP is expressed as

$$P' = \mathbf{y}^H \mathbf{S}_y^{-1} \mathbf{y} \quad (3.20)$$

where  $\mathbf{S}_y = \mathbf{Y}\mathbf{Y}^H$ . Next, we use a Householder transformation defined by  $\mathbf{A} = \mathbf{I} - 2 \frac{\mathbf{u}\mathbf{u}^H}{\mathbf{u}^H \mathbf{u}}$ , where  $\mathbf{u} = \mathbf{y} - \|\mathbf{y}\| \mathbf{e}$  and  $\mathbf{e} = [100 \dots 0]^T$ , so that  $\tilde{\mathbf{y}} = \mathbf{A}\mathbf{y} = \|\mathbf{y}\| \mathbf{e}$ . Also, let  $\tilde{\mathbf{Y}} = \mathbf{A}\mathbf{Y}$ . Since  $\mathbf{A} = \mathbf{A}^H$  and  $\mathbf{A}\mathbf{A}^H = \mathbf{A}^H \mathbf{A} = \mathbf{I}$ , it follows that the statistics of  $\tilde{\mathbf{Y}}$  are identical to that of  $\mathbf{Y}$ . Consequently, the normalized GIP is expressed as

$$P' = \tilde{\mathbf{y}}^H \mathbf{S}_{\tilde{y}}^{-1} \tilde{\mathbf{y}} \quad (3.21)$$

where  $\mathbf{S}_{\tilde{y}} = \tilde{\mathbf{Y}}\tilde{\mathbf{Y}}^H$ . Furthermore, we partition  $\tilde{\mathbf{Y}}$  as

$$\tilde{\mathbf{Y}} = \begin{bmatrix} \tilde{\mathbf{y}}_1^H \\ \tilde{\mathbf{Y}}_{11}^H \end{bmatrix} \quad (3.22)$$

where  $\tilde{\mathbf{y}}_1^H$  is the the first row of  $\tilde{\mathbf{Y}}$  and  $\tilde{\mathbf{Y}}_{11}^H$  denotes the  $(M-1) \times K$  matrix formed from the remaining rows of  $\tilde{\mathbf{Y}}$ . Consequently,  $\mathbf{S}_{\tilde{y}}$  is expressed as

$$\mathbf{S}_{\tilde{y}} = \begin{bmatrix} \tilde{\mathbf{y}}_1^H \tilde{\mathbf{y}}_1 & \tilde{\mathbf{y}}_1^H \tilde{\mathbf{Y}}_{11} \\ \tilde{\mathbf{Y}}_{11}^H \tilde{\mathbf{y}}_1 & \tilde{\mathbf{Y}}_{11}^H \tilde{\mathbf{Y}}_{11} \end{bmatrix}. \quad (3.23)$$

The inverse of  $\mathbf{S}_{\tilde{y}}$  admits a representation of the form

$$\mathbf{S}_{\tilde{y}}^{-1} = \begin{bmatrix} \mathbf{S}^{11} & \mathbf{S}^{12} \\ \mathbf{S}^{21} & \mathbf{S}^{22} \end{bmatrix} \quad (3.24)$$

Finally, the normalized GIP is expressed as

$$P' = \|\mathbf{y}\|^2 \mathbf{S}^{11}. \quad (3.25)$$

However, from the matrix inversion Lemma it follows that  $\mathbf{S}^{11} = [\tilde{\mathbf{y}}_1^H \mathbf{P}_\perp \tilde{\mathbf{y}}_1]^{-1}$ , where  $\mathbf{P}_\perp = [\mathbf{I} - \tilde{\mathbf{Y}}_{11} (\tilde{\mathbf{Y}}_{11}^H \tilde{\mathbf{Y}}_{11})^{-1} \tilde{\mathbf{Y}}_{11}^H]$ . Since  $\tilde{\mathbf{Y}}_{11} (\tilde{\mathbf{Y}}_{11}^H \tilde{\mathbf{Y}}_{11})^{-1} \tilde{\mathbf{Y}}_{11}^H$  is a projection matrix of rank  $M-1$ , it follows that  $\mathbf{P}_\perp$  is a projection matrix of rank  $K-M+1$ . Consequently,  $\tilde{\mathbf{y}}_1^H \mathbf{P}_\perp \tilde{\mathbf{y}}_1 =$

$\sum_{i=1}^{K-M+1} |\tilde{y}_1(i)|^2$ . Therefore,  $\mathbf{S}^{11}$  is simply the reciprocal of a chi-squared distributed random variable with  $K-M+1$  complex degrees of freedom. Also,  $\|\mathbf{y}\|^2$  is simply the sum of the squared magnitudes of  $M$  iid  $\text{CN}(0,1)$  random variables and hence follows a chi-squared distribution with  $M$  complex degrees of freedom. Consequently, the GIP admits a representation of the form of (3.7).